Characterization and Proteome of Circulating Extracellular Vesicles as Potential Biomarkers for NASH

Davide Povero,[1] Hirokazu Yamashita,[1] Wenhua Ren,[2] Mani G. Subramanian,[3] Robert P. Myers,[3] Akiko Eguchi,[1] Douglas A. Simonetto,[4] Zachary D. Goodman,[5] Stephen A. Harrison,[6] Arun J. Sanyal,[7] Jaime Bosch ,[8,9] and Ariel E. Feldstein[1]

Nonalcoholic fatty liver disease (NAFLD) is currently one of most common forms of chronic liver disease globally. NAFLD represents a wide spectrum of liver involvement from nonprogressive isolated steatosis to nonalcoholic steatohepatitis (NASH), characterized by liver necroinflammation and fibrosis and currently one of the top causes of end-stage liver disease and hepatocellular carcinoma. At present, there is a lack of effective treatments, and a central barrier to the development of therapies is the requirement for an invasive liver biopsy for diagnosis of NASH. Discovery of reliable, noninvasive biomarkers are urgently needed. In this study, we tested whether circulating extracellular vesicles (EVs), cell-derived small membrane-surrounded structures with a rich cargo of bioactive molecules, may serve as reliable noninvasive "liquid biopsies" for NASH diagnosis and assessment of disease severity. Total circulating EVs and hepatocyte-derived EVs were isolated by differential centrifugation and size-exclusion chromatography from serum samples of healthy individuals, patients with precirrhotic NASH, and patients with cirrhotic NASH. EVs were further characterized by flow cytometry, electron microscopy, western blotting, and dynamic light scattering assays before performing a proteomics analysis. Our findings suggest that levels of total and hepatocyte-derived EVs correlate with NASH clinical characteristics and disease severity. Additionally, using proteomics data, we developed understandable, powerful, and unique EV-based proteomic signatures for potential diagnosis of advanced NASH. *Conclusion:* Our study shows that the quantity and protein constituents of circulating EVs provide strong evidence for EV protein–based liquid biopsies for NAFLD/NASH diagnosis. (*Hepatology Communications* 2020;4:1263-1278).

Nonalcoholic fatty liver disease (NAFLD) has evolved to represent the most common cause of chronic liver disease globally.[1] Today, NAFLD is a leading indication for liver transplantation and a major etiology for hepatocellular carcinoma (HCC) in the United States.[2-4] NAFLD is characterized by the excess accumulation of lipids within the liver, typically in individuals with the metabolic syndrome, which encompasses obesity, insulin resistance, and dyslipidemia. The spectrum of NAFLD ranges from isolated steatosis, which has a benign nonprogressive course, to nonalcoholic steatohepatitis (NASH), which is characterized by the presence of hepatic necroinflammation and hepatocyte ballooning and is associated with fibrosis progression and pathological angiogenesis.[5,6] Although patients

Abbreviations: ASGPR1, asialoglycoprotein receptor 1; AUROC, area under the receiver operating characteristic curve; CI, confidence interval; ELF, Enhanced Liver Fibrosis; EV, extracellular vesicle; FC, fold change; FITC, fluorescein isothiocyanate; HCC, hepatocellular carcinoma; HVPG, hepatic venous pressure gradient; ICAM2, intercellular cell adhesion molecule 2; IL27RA, interleukin-27RA; kTSP, k top scoring pair; NAFLD, nonalcoholic fatty liver disease; NAS, NAFLD activity score; NASH, nonalcoholic steatohepatitis; RGMA, repulsive guidance molecule A precursor; STK16, serine/threonine protein kinase; TEM, transmission electron microscopy; TSG101, tumor susceptibility gene 101; vWF, von Willebrand factor; WISP1, Wnt1-inducible signaling pathway protein-1.

Received February 13, 2020; accepted May 11, 2020.

Additional Supporting Information may be found at onlinelibrary.wiley.com/doi/10.1002/hep4.1556/suppinfo.

Supported by Gilead Sciences and the National Institute of Diabetes and Digestive and Kidney Diseases (R01 DK113592).

with NAFLD may not develop NASH, patients with advanced NASH likely develop fibrosis and cirrhosis, end-stage liver disease, and HCC. NASH is currently a leading cause of end-stage liver disease and HCC in the United States, and reliable, surrogate diagnostic biomarkers for advanced NASH are urgently needed.[7] There is currently a lack of effective treatments, and great efforts are underway to develop pharmacological interventions for patients with NASH and fibrosis. At present, the only reliable method of differentiating fibrotic precirrhotic NASH from cirrhotic NASH is liver biopsy. However, this procedure is invasive and prone to complications such as bleeding,[8] is associated with sampling variability and limited representation of the whole liver (only 1/50,000 of the liver volume), is difficult to repeat to monitor changes in liver injury over time, and is associated with underestimation of disease severity. With the anticipated development of drug therapies for NASH, noninvasive alternatives to liver biopsy, to identify those patients who require intervention and follow these patients to monitor therapeutic responses, are urgently needed.[9] In this study, we evaluated the ability of circulating extracellular vesicles (EVs)[10] and their unique protein composition as noninvasive biomarkers for diagnosis and potential assessment of prognosis in patients with advanced NASH compared to healthy control subjects. Circulating EVs are cell-derived, nanosize and microsize membrane–surrounded structures containing a specific cargo from the cell of origin. EVs can be detected abundantly in several body fluids,[11] emphasizing their potential utility as noninvasive liquid biopsies.[12] We previously showed that in experimental models of NASH, liver and blood levels of EVs are increased and correlate with changes in liver histology.[13] An in-depth characterization of the EV cargo through proteomic analysis also identified a signature that reliably differentiates NASH animals from controls.[13] In this human study we isolated circulating EVs from healthy control subjects, histologically confirmed patients with precirrhotic NASH, and patients with cirrhotic NASH. After a complete characterization of EV structural features, we showed that differences in the quantity and protein constituents of circulating EVs enable the differentiation of patients with NASH from healthy control individuals, as well as patients with precirrhotic NASH from patients with cirrhotic NASH.

DOI 10.1002/hep4.1556

Potential conflict of interest: Dr. Subramanian owns stock in Gilead. Dr. Sanyal consults and received grants from Conatus, Gilead, Echosens-Sandhill, malinckrodt, Salix, Novartis, Galectin, and Sequana. He consults and owns stock in GenFit, Hemoshear, Durect, and Indalo. He consults for Immuron, Intercept, Pfizer, Boehringer Ingelheim, Nimbus, Lilly, Merck, Novo Nordisk, Fractyl, Allergan, Chemomab, Affimmune, Teva, Aredlyx, Terns, ENYO, Birdrock, Albireo, Sanofi, Takeda, Janssen, Zydus, BASF, AMRA, Perspectum, Owl, Poxel, Servier, Second Genome, General Electric, and 89 Bio. He received grants from Bristol-Myers Squibb. He received royalties from Elsevier and Uptodate. He owns stock in Exhalenz, Akarna, and Tiziana. He is employed by Sanyal Bio. Dr. Bosch consults for Gilead. Dr. Myers is employed by and owns stock in Gilead. Dr. Harrison owns stock, consults for, advises, and received grants from Cirius, Galectin, Genfit, Madrigal, Metacrine, NGM Bio, and North Sea. He owns stock in, consults for, and advises Akero and HistoIndex. He consults for, advises, and received grants from Axcella, CiVi Biopharma, CymaBay, Galmed, Gilead, HighTide, Hepion, Intercept, Novartis, Novo Nordisk, Sagimet, and Viking. He consults for and advises Altimmune, Blade Therapeutics, CLDF, Echosens, Forsite Labs, Gelesis, Indalo, Innovate, Medpace, Perspectum, Poxel, Prometic, Ridgeline Therapeutics, and Terns. He received grants from Axcella, BMS, Conatus, Enyo, Genetech, Immuron, Pfizer, Second Genome, Tobira, and Allergan.

ARTICLE INFORMATION:

From the [1]Department of Pediatrics, University of California San Diego, La Jolla, CA; [2]Genomics and Microarray Core, University of Colorado Denver, Aurora, CO; [3]Gilead Sciences, Inc., Foster City, CA; [4]Department of Gastroenterology and Hepatology, Mayo Clinic, Rochester, MN; [5]Inova Fairfax Hospital, Falls Church, VA; [6]Pinnacle Clinical Research, San Antonio, TX; [7]Virginia Commonwealth University, Richmond, VA; [8]Inselspital, Bern University, Bern, Switzerland; [9]Ciberehd-Idibaps, University of Barcelona, Barcelona, Spain.

ADDRESS CORRESPONDENCE AND REPRINT REQUESTS TO:

Ariel E. Feldstein, M.D.
Department of Pediatrics, Division of Pediatric Gastroenterology Hepatology and Nutrition, University of California San Diego
3020 Children's Way, MC 5030
San Diego, CA 92103-8450
E-mail: afeldstein@ucsd.edu
Tel.: +1-(858) 966-8907

Materials and Methods

PATIENT SAMPLES

Baseline serum samples were collected from 25 patients with precirrhotic NASH with F3 fibrosis and 25 patients with cirrhotic NASH with F4 fibrosis, who participated in phase 2 randomized trials evaluating the safety and efficacy of simtuzumab versus placebo (Clinicaltrials.gov NCT01672866 and NCT01672879).[14] As controls, the serum from 25 healthy subjects who participated in pharmacokinetics and phase 1 trials were evaluated. Further information can be found in the Supporting Information.

STUDY ASSESSMENTS

Liver histologic assessments were performed as previously described.[14] Further information on liver biopsies assessments is provided in the Supporting Information.

ISOLATION AND CHARACTERIZATION OF CIRCULATING EXTRACELLULAR VESICLES

Circulating EVs were isolated from serum samples by differential centrifugation and by size exclusion chromatography, as previously described.[15] Circulating EV identification and quantitation was performed using the BD LSRII Flow Cytometer System (BD Biosciences, San Jose, CA), and the data were analyzed using FlowJo software (TreeStar Inc., Ashland, OR), as previously described.[13] Further information on EV isolation and characterization is provided in the Supporting Information.

PROTEIN ISOLATION AND WESTERN BLOTTING

Purified circulating EV proteins were extracted through five freeze/thaw cycles, which result in greater concentration of extracts and enrichment of low abundant proteins. Protein concentration was determined by micro BCA protein assay kit (catalog #23235; Thermo Scientific, Waltham, MA), according to the manufacturer's instructions. Further information can be found in the Supporting Information.

SOMAscan PROTEOMICS ARRAY AND DATA ANALYSIS

The protein cargoes of EVs were determined in purified isolated circulating EVs from healthy controls,[16] patients with precirrhotic (F3) NASH, and patients with cirrhosis (F4) due to NASH by SOMAscan protein array (SomaLogic, Boulder, CO), which included 1,345 unique proteins. Further information can be found in the Supporting Information.

DEVELOPMENT OF A REPRODUCIBLE EV PROTEIN–BASED SIGNATURE

To explore prognostic EV protein markers for NASH, we trained and validated a parameter-free classifier called "k top scoring pair" (kTSP)[17,18] using a training data set and a validation data set. Further information can be found in the Supporting Information.

EVALUATION OF THE PERFORMANCE OF kTSP CLASSIFICATION

The performance of the classification is evaluated by the area under the receiver operating characteristic curve (AUROC) using the kTSP classifier built with training data and the threshold selected to achieve the best classification accuracy. Further information can be found in the Supporting Information.

PAIRWISE COMPARISONS OF EVs IN A VALIDATION STUDY

Pairwise comparisons were generated for the top expressed proteins in the validation study comparing all three cohorts. Further information can be found in the Supporting Information.

STATISTICAL ANALYSIS

Excluding the proteomics data, which were analyzed differently as reported previously, all other data were expressed as the mean ± SD unless otherwise indicated. Differences among three or more groups

were compared by a nonparametric Kruskal-Wallis analysis of variance test. Further information on the statistical analysis can be found in the Supporting Information.

Results

CIRCULATING EVs CAN BE IDENTIFIED AND CHARACTERIZED IN THE SERA OF NASH PATIENTS

Circulating EVs isolated from plasma and serum have been proposed as "liquid biopsies" for several diseases.[12,19-22] Tumor-EVs isolated from the sera of patients with tumor glioblastoma showed robust performance in providing diagnostic information and aid in therapeutic decisions for patients with cancer through a blood test.[10,23] Based on these reports, we investigated whether hepatocyte-derived EVs could serve as prognostic and diagnostic biomarkers for advanced NASH. To address this hypothesis, we isolated circulating EVs from patients with precirrhotic NASH (n = 25), patients with cirrhotic NASH (n = 25), and healthy control subjects (n = 25), as detailed in Table 1. Total circulating EVs were isolated and purified by differential centrifugation followed by size-exclusion chromatography, to separate EVs from circulating serum proteins, contaminants and lipoproteins, particularly high-density lipoproteins (Fig. 1A). Pure circulating EVs from each group were further characterized and quantified. We first grouped all NASH samples and compared the EV levels with those in healthy controls. Flow cytometry analyses identified a significantly higher number of total calcein–fluorescein isothiocyanate (FITC)+ circulating EVs in NASH samples compared with healthy controls (Fig. 1B). The average circulating EV size did not differ between NASH and healthy control samples (Fig. 1C). EVs were further characterized using transmission electron microscopy (TEM). TEM identified a large heterogeneous population of circulating EVs in both NASH and healthy control samples, and no specific EV morphological features were found to be present among study groups (Fig. 1D). Previously established circulating EV protein markers[24] were identified through western blot analysis and included Alix, CD63, and TSG101 (tumor susceptibility gene 101) (Fig. 1E). TSG101 (ESCRT-I protein tumor susceptibility gene 101) plays a role in EV synthesis and secretion,[25] particularly by damaged cells, which normally secrete higher levels of EVs. Our data indicate that in patients with advanced fibrosis due to NASH, EVs are secreted into the blood stream and can be isolated and characterized based on their molecular and physical properties.

TABLE 1. BASELINE CHARACTERISTICS OF THE STUDY POPULATION

		Total (n = 50)
Demographics	Age, years	55 (48-58)
	Female	68% (34)
	Body mass index, kg/m^2	33 (29-37)
Liver biochemistry	Alanine aminotransferase, U/L	40 (29-73)
	Alkaline phosphatase, U/L	78 (65-106)
	Gamma-glutamyl transferase, U/L	59 (31-108)
	Bilirubin, mg/dL	0.5 (0.4-0.7)
	INR	1.1 (1.0-1.1)
	Platelets, $\times 10^3$/μL	171 (137-240)
	MELD	7 (6-8)
Fibrosis markers	NAFLD Fibrosis Score	0.14 (–0.95 to 1.22)
	FibroSURE	0.43 (0.22-0.77)
	ELF Test	10.0 (9.3-10.7)
Histology	NAS ≥ 4	73% (36/49)
	Cirrhosis (Ishak 5-6)	50% (25)
Portal pressure	HVPG	11.5 (8.5-15.5)
	CSPH (HVPG ≥ 10 mm Hg)	52% (13)

Note: All data are presented as the median (interquartile range) or percentage (n). HVPG was measured only in subjects with cirrhosis. Abbreviations: CSPH, clinically significant portal hypertension; INR, international normalized ratio; and MELD, Model for End-Stage Liver Disease.

LEVELS OF HEPATOCYTE-DERIVED EVs ARE ASSOCIATED WITH NASH CHARACTERISTICS AND CORRELATE WITH DISEASE SEVERITY

To determine whether the amount of total circulating EVs could discriminate between different stages of NASH, we measured EV levels separately in both the precirrhotic NASH cohort as well as the cirrhotic NASH cohort, and we compared the results with the healthy control samples. Our data show that the median level of EVs was not significantly greater in patients with precirrhotic NASH compared with

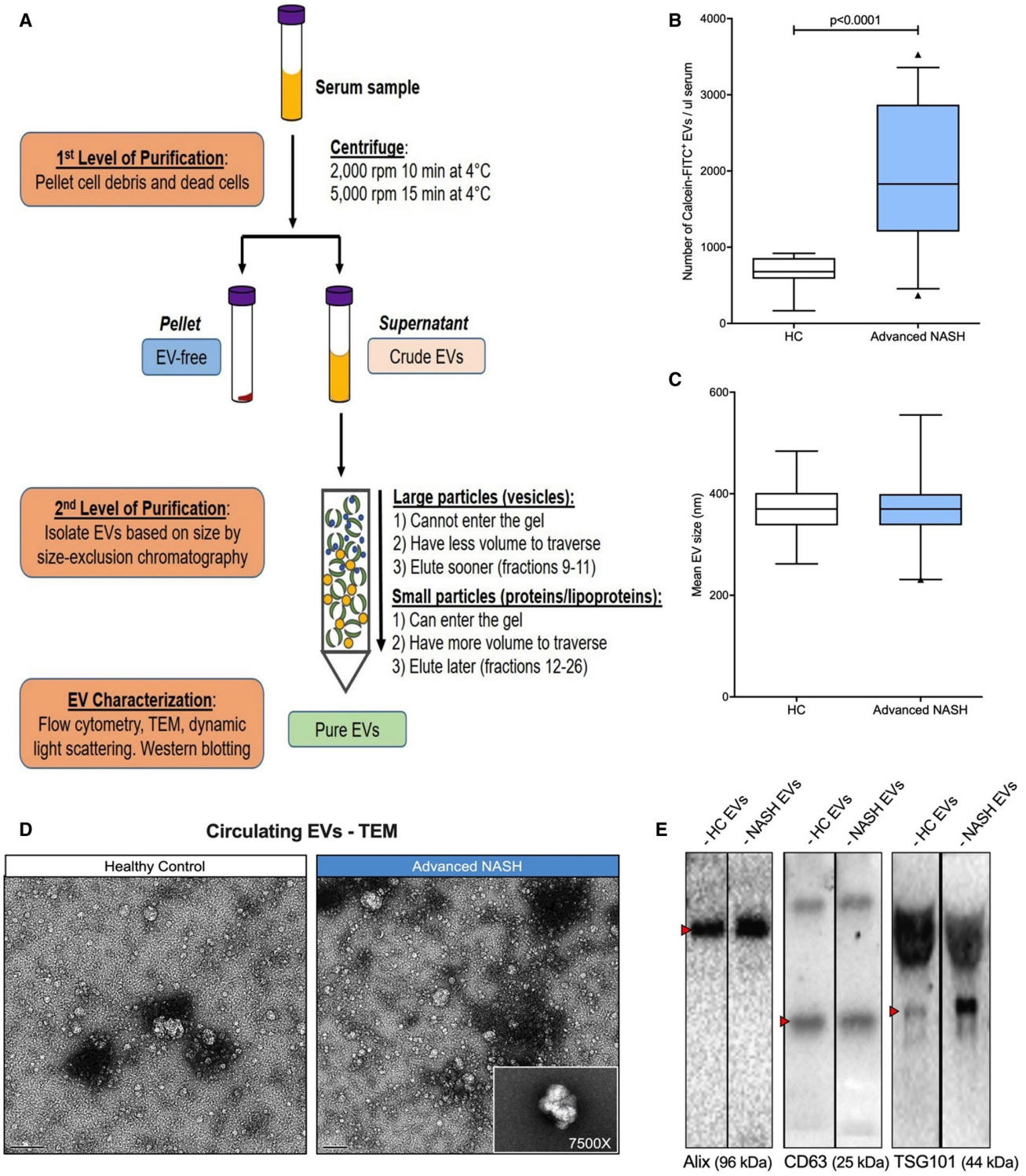

FIG. 1. Isolation, detection, and characterization of circulating EVs in serum samples of patients with NASH. (A) Flow chart of circulating EV isolation. (B) Number of calcein/FITC+ circulating EVs detected by flow cytometry in healthy controls (n = 11) or liver biopsy–proven patients with advanced NASH (n = 50). (C) Mean size[38] of circulating EVs measured by dynamic light scattering. (D) Representative TEM microphotographs of circulating EVs. (E) Representative western blots of EV markers Alix, CD63, and TSG101 in healthy controls and patients with advanced NASH. Values represent mean ± SD. Kruskal-Wallis test with *post hoc* Mann-Whitney U test and Bonferroni correction were used for statistical analysis. Abbreviation: HC, healthy control.

healthy controls, whereas the median EV level was significantly higher in patients with cirrhotic NASH compared with healthy controls (Fig. 2A). This suggests that disease severity and progression are associated with greater EV secretion from damaged cells. Compared to total EVs, tissue-specific or cell-specific circulating EVs may represent a stronger indicator of a disease pathophysiological status and may provide important and unique information on the injured tissue or a specific pathophysiological process. For this reason, we examined two hepatocyte-specific markers in circulating EVs: the bile acyl–coenzyme A synthetase (SLC27A5) and the asialoglycoprotein receptor 1 (ASGPR1). Our data indicate that approximately 20% of total circulating EVs expressed hepatocyte-specific markers. Median levels of SLC27A5-positive EVs were 3-4-fold greater in subjects with NASH compared to healthy controls; no significant difference was noted between the two NASH cohorts (Fig. 2B). Expression of SLC27A5 is up-regulated in fat-laden hepatocytes, as this enzyme plays a crucial role in fatty acid uptake, elongation, and synthesis. On the other hand, SLC27A5 expression is down-regulated during the progression from NASH to cirrhosis, likely as a result of fat loss occurring during the late stage of the disease.[26] These findings suggest that SLC27A5 may be a specific marker of fat-laden hepatocyte-EVs of NAFLD and NASH livers, but not of hepatocyte-EVs of cirrhotic livers, which instead contain ASGPR1, whose expression is independent of fatty acid homeostasis. Levels of ASGPR1-positive EVs increased with disease severity, almost doubling in precirrhotic NASH and increasing three-fold in cirrhotic NASH compared with healthy controls (Fig. 2C). To further test the diagnostic ability of hepatocyte-derived EVs, we determined associations between the number of EVs with key serological, histological, and hemodynamic features of disease severity, including liver biochemistries, NAFLD activity score (NAS), fibrosis stage, hepatic collagen content, α-smooth muscle actin expression by morphometry, serum fibrosis markers, and in patients with cirrhotic NASH, the hepatic venous pressure gradient (HVPG). Although the number of EVs did not correlate with demographic features, liver biochemistry, NAFLD activity score, fibrosis markers, HVPG or Model for End-Stage Liver Disease score (data not shown), the number of hepatocyte-derived, circulating EVs correlated with fibrosis stage, FibroTest, Enhanced Liver Fibrosis (ELF) test, NAFLD Fibrosis Score, bilirubin, and platelet count (Table 2). Moreover, a statistically significant correlation between the number of hepatocyte-derived circulating EVs and values of HVPG in patients with cirrhosis was observed (Fig. 2E). Indeed, patients with clinically significant portal hypertension (HVPG ≥ 10 mmHg) had more hepatocyte-derived circulating EVs than patients with HVPG below 10 mmHg (Fig. 2D). We also tested the ability of hepatocyte-derived EVs to accurately and noninvasively predict clinically significant portal hypertension in patients with cirrhotic NASH, as an alternative to invasive HVPG measurement. Our analysis indicates that the hepatocyte-derived EV cutoff of at least 668 EVs/μL serum exhibits sensitivity of 92% and specificity of 75% for differentiating patients with and without clinically significant portal hypertension (AUROC: 0.79; 95% confidence interval [CI]: 0.589-0.988) (Fig. 2F). In summary, these findings indicate that a subpopulation of circulating EVs identified in patients with NASH are released by hepatocytes and that that hepatocyte-specific EVs strongly correlate with clinical features of NASH severity.

PROTEOMICS ANALYSIS OF CIRCULATING EVs IDENTIFIES DIFFERENTIALLY EXPRESSED PROTEINS IN HEALTHY CONTROLS, PRECIRRHOTIC NASH, AND CIRRHOTIC NASH SAMPLES

Extensive published studies have demonstrated the presence of abundant proteins, among other bioactive molecules, encapsulated in EVs.[27] Analyzing EV protein composition may identify disease-specific or disease stage–specific proteins highly enriched in EVs that may provide protein signatures for disease diagnosis. As a consequence, we decided to determine the circulating EV proteome, applying an unsupervised comprehensive proteomics approach. Lysates of purified circulating EVs isolated from seven randomly selected healthy control, precirrhotic NASH, and cirrhotic NASH samples were used for an initial discovery study using the SOMAscan protein array (SomaLogic, Boulder, CO), which included 1,345 unique proteins. The results of this discovery

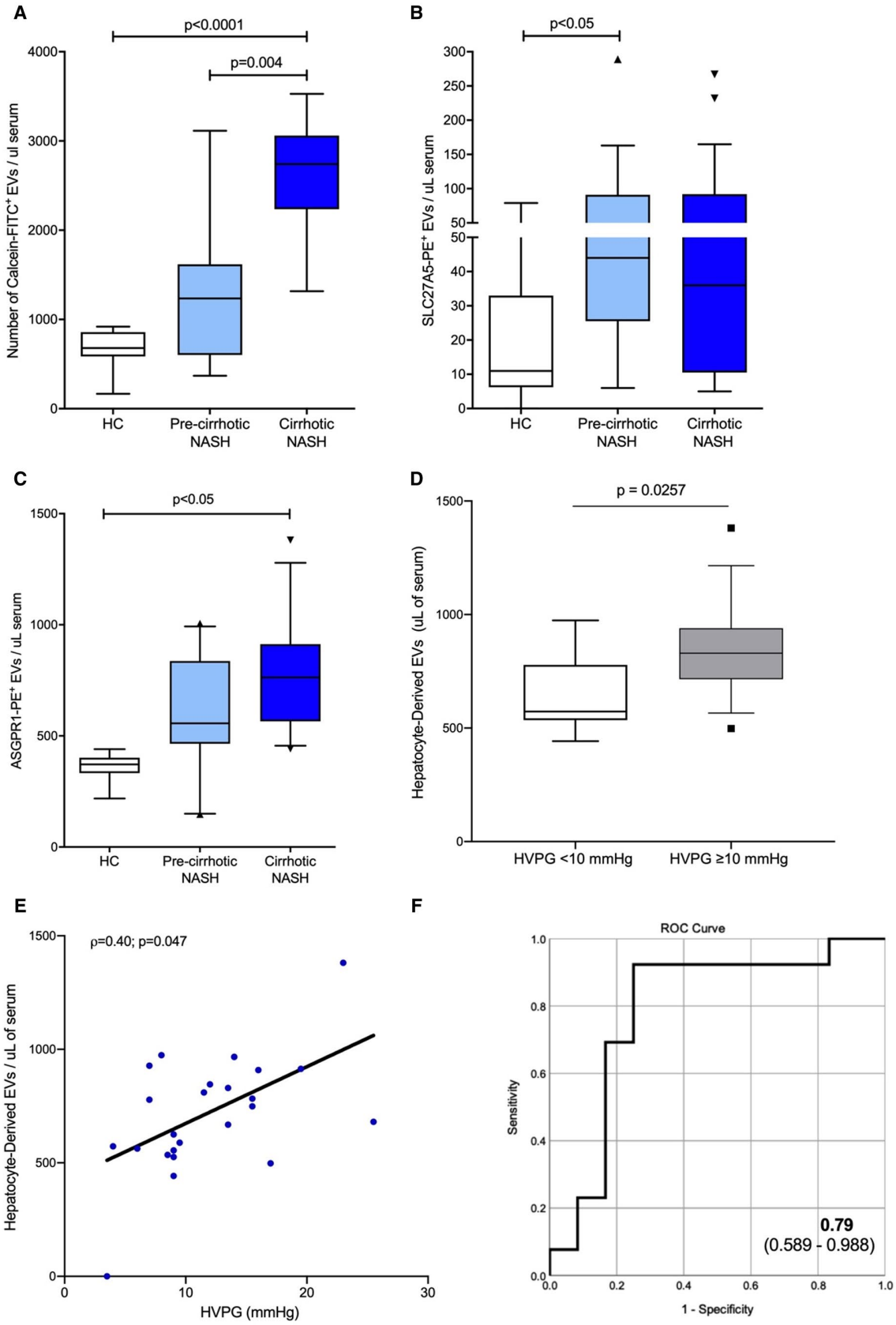
A
p<0.0001
p=0.004
Number of Calcein-FITC+ EVs / ul serum
4000
3000
2000
1000
0
HC
Pre-cirrhotic NASH
Cirrhotic NASH
B
p<0.05
SLC27A5-PE+ EVs / uL serum
300
250
200
150
100
50
40
30
20
10
0
HC
Pre-cirrhotic NASH
Cirrhotic NASH
C
p<0.05
ASGPR1-PE+ EVs / uL serum
1500
1000
500
0
HC
Pre-cirrhotic NASH
Cirrhotic NASH
D
p = 0.0257
Hepatocyte-Derived EVs (uL of serum)
1500
1000
500
0
HVPG <10 mmHg
HVPG ≥10 mmHg
E
ρ=0.40; p=0.047
Hepatocyte-Derived EVs / uL of serum
1500
1000
500
0
0
10
20
30
HVPG (mmHg)
F
ROC Curve
Sensitivity
1.0
0.8
0.6
0.4
0.2
0.0
0.0
0.2
0.4
0.6
0.8
1.0
1 - Specificity
0.79
(0.589 - 0.988)

FIG. 2. Levels of hepatocyte-specific circulating EVs correlate with NASH severity. (A) Number of calcein/FITC+ circulating EVs in healthy controls, patients with precirrhotic NASH, and patients with cirrhotic NASH detected by flow cytometry. (B,C) Flow cytometry analysis of hepatocyte-specific EVs either positive for hepatocyte marker SLC27A5 or ASGPR1. (D) Number of hepatocyte-specific circulating EVs in individuals with cirrhotic NASH with HVPG lower or greater than 10 mmHg, as indication of clinically significant portal hypertension. (E) Spearman correlation between hepatocyte-specific circulating EVs and HVPG levels. (F) AUROC curve for hepatocyte-derived EVs for diagnosis of portal hypertension in patients with cirrhotic NASH. Hepatocyte-EV count of 668 EVs/ μL or higher serum showed sensitivity of 92% and specificity of 75% for differentiating patients with clinically significant portal hypertension from patients with no clinically relevant portal hypertension (AUROC: 0.79; 95% CI: 0.589-0.988). Kruskal-Wallis test with *post hoc* Mann Whitney U test and Bonferroni correction were used for statistical analysis. Abbreviations: HC, healthy control; ROC, receiver operating characteristic.

TABLE 2. CORRELATION BETWEEN HEPATOCYTE-DERIVED CIRCULATING EVs AND NASH-RELATED CLINICAL VARIABLES

Variable	Spearman Correlation (ρ)	*P* Value
Fibrosis stage	0.28	0.048
NAFLD Fibrosis Score	0.29	0.047
FibroSURE	0.31	0.037
ELF test	0.28	0.056
NAS	0.05	0.737
Bilirubin, mg/dL	0.26	0.066
Platelets, $\times 10^3$/μL	–0.38	0.006
HVPG, mm Hg	0.4	0.047

Note: Levels of ASGPR1+ circulating EVs as indication of hepatocyte-specific EVs were correlated with NASH clinical variables. The associations were determined using Spearman correlations and Mann-Whitney U tests.

study identified proteins that were up-regulated or down-regulated uniquely in each of the three cohorts and other proteins that overlapped between two or more groups. Multiple comparisons of the differentially expressed proteins (DEPs) in the three groups identified 78 up-regulated and 65 down-regulated proteins in precirrhotic NASH EVs when compared with healthy control EVs, while we identified 61 up-regulated and 108 down-regulated unique proteins in precirrhotic NASH EVs compared with cirrhotic NASH EVs (Fig. 3A). Oppositely, we identified 116 up-regulated and 129 down-regulated proteins in cirrhotic NASH EVs compared with healthy control EVs, and 43 up-regulated and 18 down-regulated proteins in cirrhotic NASH EVs compared with precirrhotic NASH EVs (Fig. 3B). An unsupervised hierarchical clustering analysis of the top 50 DEPs with adjusted *P* value of 0.05 identified distinct and unique protein expression patterns particularly between healthy controls and cirrhotic NASH circulating EVs, suggesting that the protein composition of EVs is strongly associated with the severity of NASH (Fig. 3C). To graphically display all statistically significant circulating EV proteins identified in cirrhotic NASH EVs, volcano plots –log10(adj. *P* value) versus log2 fold-change of EV proteins in cirrhotic NASH versus precirrhotic NASH (Fig. 4A) and in cirrhotic NASH versus healthy controls (Fig. 4B) were constructed using a corrected *P* value of 0.05 as threshold. Points above the nonaxial horizontal line indicate a EV-protein *P* value greater than 0.005, which were down-regulated if on the left of the nonaxial vertical red line or up-regulated if on the right of the nonaxial vertical green line. Five proteins demonstrated a 0.2 or greater fold change (FC) in cirrhotic NASH versus precirrhotic NASH circulating EVs, whereas 10 proteins demonstrated a 0.2 or greater FC in cirrhotic NASH versus healthy control circulating EVs. Particularly interesting is the up-regulation of von Willebrand factor (vWF) in cirrhotic NASH circulating EVs versus healthy controls. Even when below the *P*-value threshold of 0.005 used for this analysis, vWF demonstrated a 2-FC increase in cirrhotic NASH circulating EVs registering a *P* value greater than 0.05. This protein is secreted primarily by endothelial cells and is strongly increased in serum of patients with cirrhosis. These findings may suggest a potential form of secretion of vWF by endothelial cells through EVs. We then wanted to identify distinct clusters of circulating EV proteins that could clearly distinguish the NASH patients from the healthy individuals. For this reason, we performed unsupervised hierarchical analyses of the top 50 differentially expressed proteins in cirrhotic NASH versus precirrhotic NASH or healthy control circulating EVs (Fig. 4C,D). Our proteomics data suggest that circulating EVs carry specific proteins that may provide disease and disease stage–specific multiprotein-based signatures that may be useful for diagnosis and potentially prognosis of NASH.

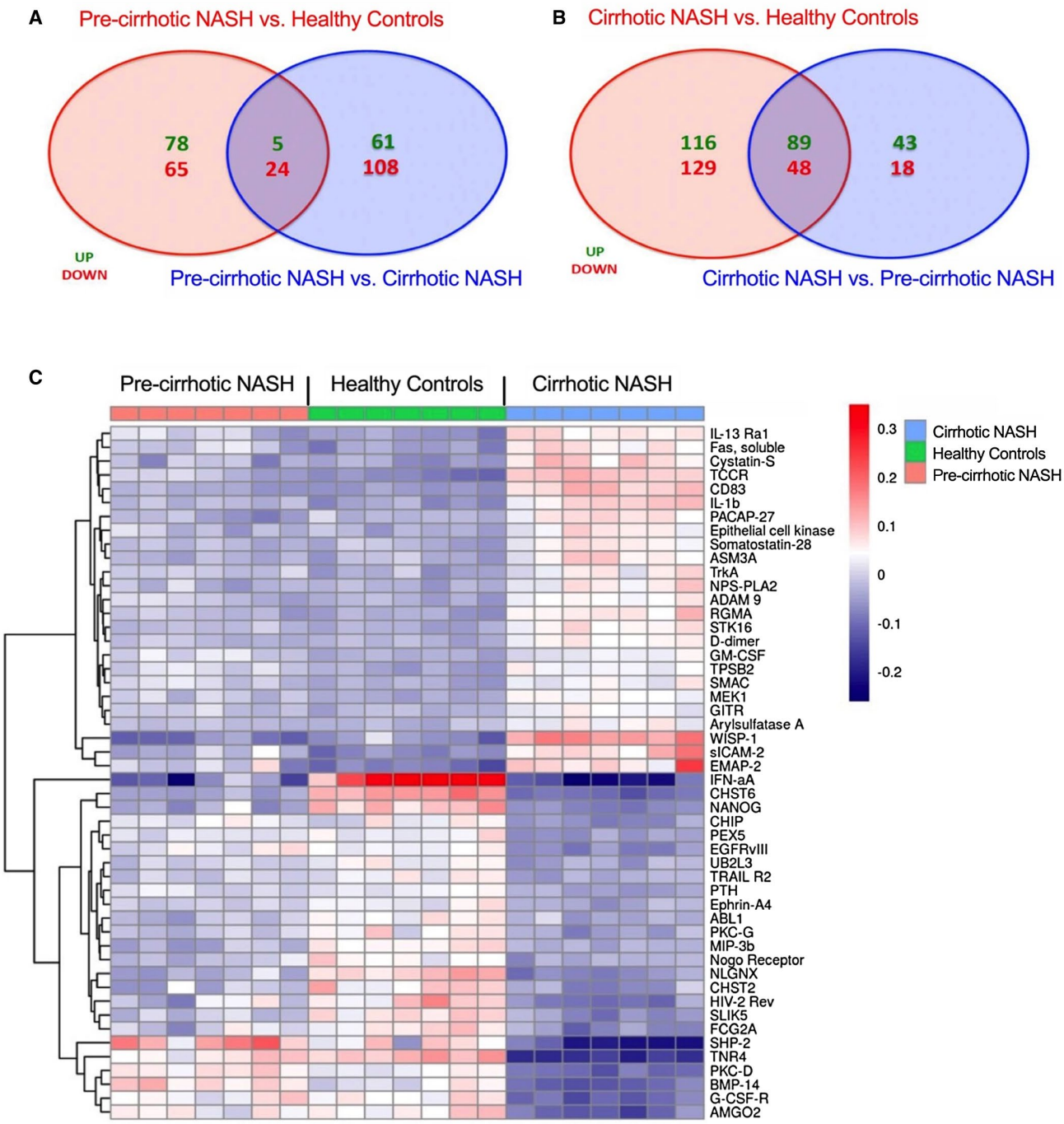

FIG. 3. Analysis of circulating EVs proteome by SOMAScan protein array in all three cohorts. (A) Venn diagram of differentially expressed EV proteins in patients with precirrhotic NASH versus healthy controls or patients with cirrhotic NASH. (B) Venn diagram of differentially expressed EV proteins in patients with cirrhotic NASH compared with healthy controls or patients with precirrhotic NASH. A cutoff of adjusted *P* value of 0.01 was used for both Venn diagrams. (C) Unsupervised hierarchical clustering analysis of the top 50 differentially expressed circulating EV proteins in patients with cirrhotic NASH versus patients with precirrhotic NASH versus healthy controls (n = 7/group). The top 50 proteins listed on the heat map were selected based on the adjusted *P* value of 0.05 from the cirrhotic NASH versus healthy controls comparison. Mean and SD of all three groups were used to normalize the expression value. The closer the color is to bright blue, the lower the expression, whereas the closer the color is to bright red, the higher the expression.

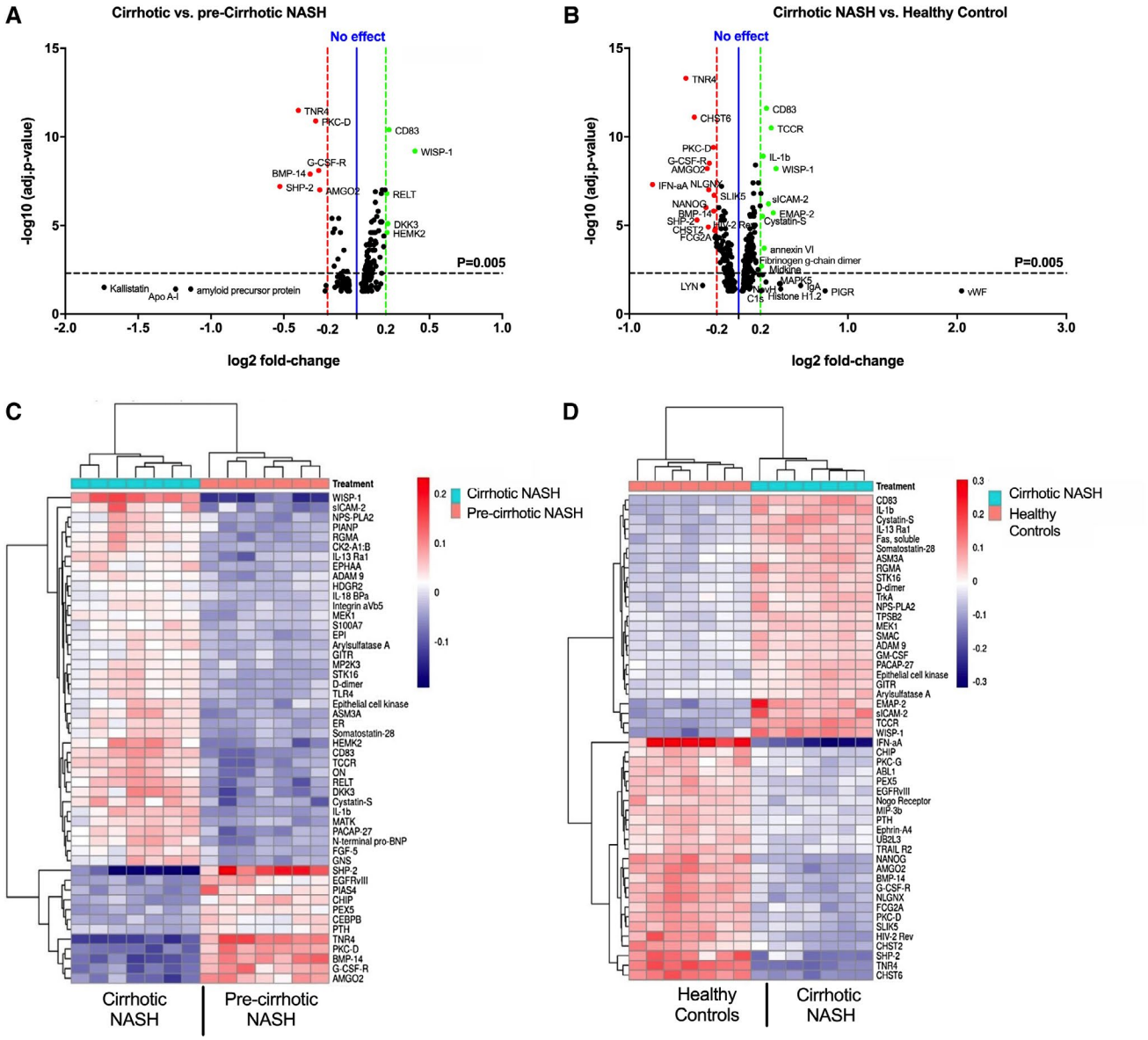

FIG. 4. Analyses of most abundant circulating EV proteins in paired comparisons. Volcano plots illustrating significantly differentially abundant EV-proteins in patients with cirrhotic NASH versus patients with precirrhotic NASH (A) and patients with cirrhotic NASH versus healthy controls (n = 7/group) (B). The -log10 (adjusted *P* value) is plotted against the log2 fold-change. The nonaxial vertical blue line denotes no effect in protein expression; green line denotes +0.2-fold change; and the red line denotes –0.2-fold change. The nonaxial black horizontal line denotes *P* value greater than 0.005, which is out of the significance threshold (before logarithmic transformation). Unsupervised hierarchical clustering analysis of the top 50 differentially expressed circulating EV proteins in patients with cirrhotic NASH versus patients with precirrhotic NASH (C) and in patients with cirrhotic NASH versus healthy controls (n = 7/group) (D). An adjusted *P* value of 0.05 was used to generate the heat maps. The closer the color is to bright blue, the lower the expression, whereas the closer the color is to bright red, the higher the expression.

DEVELOP REPRODUCIBLE SIGNATURE AND DIAGNOSTIC TEST FOR NASH THROUGH VALIDATION AND REPROCESSING OF CIRCULATING EV PROTEOMICS DATA

Currently, liver biopsy remains the gold standard for diagnosis of NASH despite its invasive nature, potential complications, and cost. Importantly, identification and validation of reliable diagnostic and prognostic biomarkers for NASH are urgently needed. A major hurdle in translating biomarker research studies into clinically useful assays is lack of reproducibility and rigorous criteria to report potential NASH biomarkers. For these reasons, in this study we aim to identify EV protein–based signatures for potential diagnosis and prognosis of advanced NASH, based on several two-protein comparisons. Specifically, our goal was to provide a transparent method through which a proteomics-based NASH stage predictor might be developed from training data and evaluated on independent test data with sufficient detail and documentation to allow the full process to be replicated by other researchers. To address this goal, we adopted an extension of kTSP to develop understandable and powerful EV-based proteomics signatures.[17] Using the top 100 proteins as input, 3 pairs were selected for the advanced NASH versus healthy controls comparison (Fig. 5A), and 12 pairs were selected for the precirrhotic NASH versus cirrhotic NASH comparison, from 2 to 50 pairs (Fig. 5C). To better illustrate which feature pairs are promising for classification among three combinations of precirrhotic NASH, cirrhotic NASH or healthy controls, we generated the corresponding heat maps (Fig. 5A,C). Analyses of the performance of the classification showed that the AUROC of the classifier for advanced NASH versus healthy controls was 0.77 (UB2L3 > Fas, soluble pair) and showed a good separation between advanced NASH and healthy controls (blue squares assigned to healthy controls, red squares assigned to advanced NASH) with sensitivity of 75%, specificity of 83%, and accuracy of 77% (Fig. 5B). For the precirrhotic NASH versus cirrhotic NASH comparison, the best accuracy was achieved by two feature pairs (IL13Ra1 > TNR4; WISP-1 > BMP-14) and showed an accuracy of 80%, sensitivity of 80%, and specificity of 80% (Fig. 5D). These protein pair(s) have strong predictive power for liver fibrosis or cirrhosis disease classification, and confirmatory studies by other protein assay platforms in additional data sets will help to validate our findings. To further strengthen our findings, we decided to adopt a multibiomarker approach consisting of identifying a panel of EV-encapsulated proteins that may be used as disease-specific signatures to diagnose advanced NASH. Specifically, we performed an independent validation study by repeating the SOMAscan protein array on a new group of 10 randomly selected circulating EV samples from precirrhotic NASH and cirrhotic NASH and 6 from healthy controls. Using statistical pairwise comparisons, we assessed the validity of identified circulating EV protein signatures by authenticating their correlation with histological assessment of advanced NASH. Expression levels of the top seven most expressed circulating EV proteins in cirrhotic NASH samples (WISP1 [Wnt1-inducible signaling pathway protein-1], aminoacyl-tRNA synthetase interacting multifunctional protein 1 [AIMP1], IL27RA [interleukin-27RA], ICAM2 [intercellular cell adhesion molecule 2], IL1β [interleukin-1β], STK16 [serine/threonine protein kinase], and RGMA [repulsive guidance molecule A precursor]) were compared in precirrhotic NASH versus healthy controls, cirrhotic NASH versus healthy controls, and cirrhotic NASH versus precirrhotic NASH. Interestingly, our analyses show a clear separation in distribution of all seven proteins, particularly in the cirrhotic NASH versus healthy controls and in cirrhotic NASH versus precirrhotic NASH cohort comparisons (Fig. 6A-G). Among all comparisons, the distribution of some proteins separated particularly well in the two cohorts. These include WISP1, with a FC of 1.26 in cirrhotic NASH versus healthy controls and 1.32 in cirrhotic NASH versus precirrhotic NASH (Fig. 6A); AIMP1, with a FC of 1.24 in cirrhotic NASH versus healthy controls and 1.12 in cirrhotic NASH versus precirrhotic NASH (Fig. 6B); and IL27RA, with a FC of 1.23 in cirrhotic NASH versus healthy controls and 1.14 in cirrhotic NASH versus precirrhotic NASH (Fig. 6C). Our findings confirm that protein EV–based signatures may have utility as tools to diagnose patients with NASH.

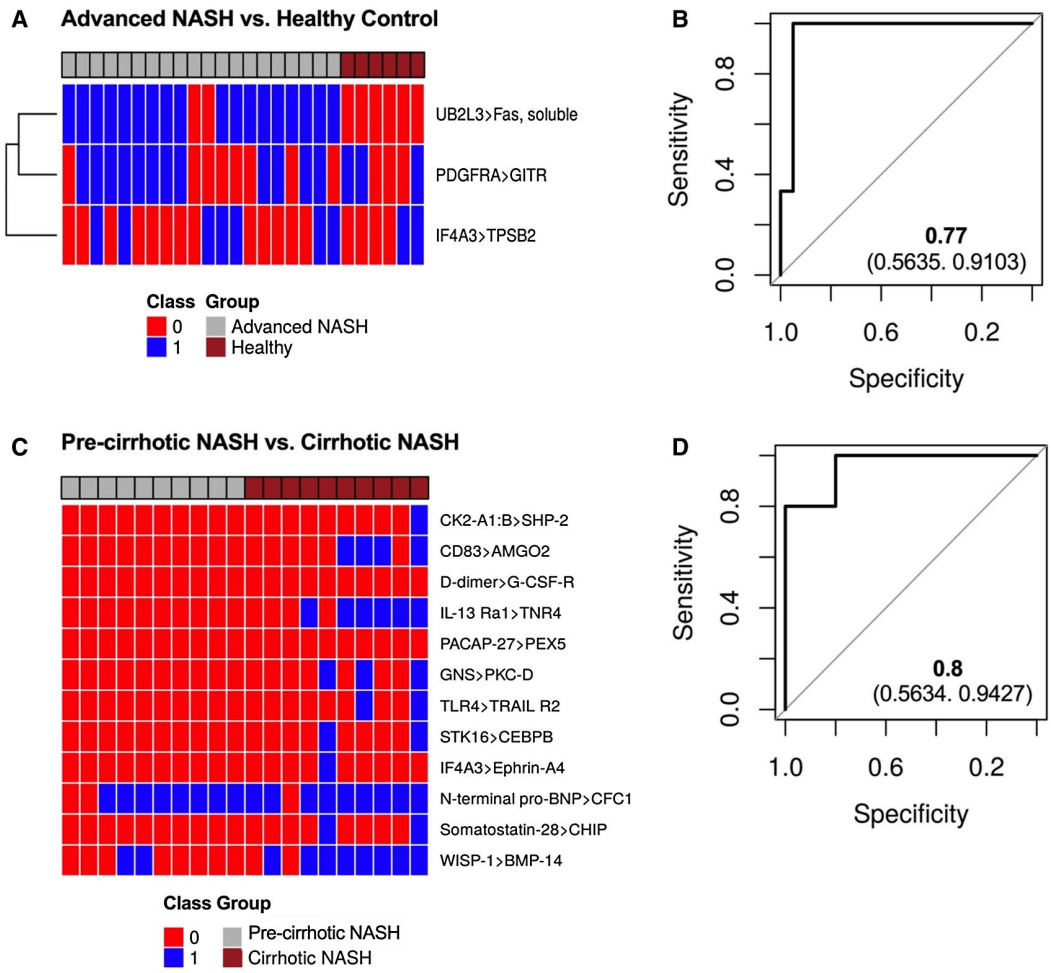

FIG. 5. Performance of circulating EV protein signatures for identification of healthy controls, patients with precirrhotic NASH, or patients with cirrhotic NASH. (A) kTSP votes training heat map of the k-top performing pairs of circulating EV proteins identified in patients with advanced NASH versus healthy controls during the validation study. The 20 gray boxes correspond to 10 patients with precirrhotic NASH and 10 patients with cirrhotic NASH grouped into one advanced NASH data set, while the red boxes correspond to the 6 healthy controls. (B) AUROC of kTSP-selected top performing pairs of circulating EV proteins identified in patients with advanced NASH versus healthy controls (AUROC: 0.77; 95% CI: 0.5635-0.9103). (C) kTSP votes training heat map of the top performing pairs of circulating EV proteins identified in patients with precirrhotic NASH versus patients with cirrhotic NASH during the validation study. Gray and red boxes correspond to each of the 10 patients in the two groups. (D) AUROC of kTSP-selected top performing pairs of circulating EV proteins identified in patients with precirrhotic NASH versus patients with cirrhotic NASH (AUROC: 0.8; 95% CI: 0.5634-0.9427). A cutoff value equal to the number of kTPS pairs observed in each group was adopted.

Discussion

The findings of this study show that circulating EVs can be isolated and characterized from the serum samples of patients with different stages of NASH. EVs are membrane-surrounded structures potentially released from every cell in the extracellular environment. Based on their biogenesis, composition and size, EVs can be classified as small vesicles or exosomes (30-150 nm in diameter), which are released by exocytosis following fusion of multivesicular bodies with the plasma membrane, and large vesicles or microvesicles (150-1,000 nm in diameter), which are released by controlled budding of the plasma membrane.[28] In general, EVs can serve autocrine and paracrine functions by shuttling a variety of bioactive molecules, including noncoding RNAs, proteins, lipids, and nuclei acids.[29] Although previous studies reported

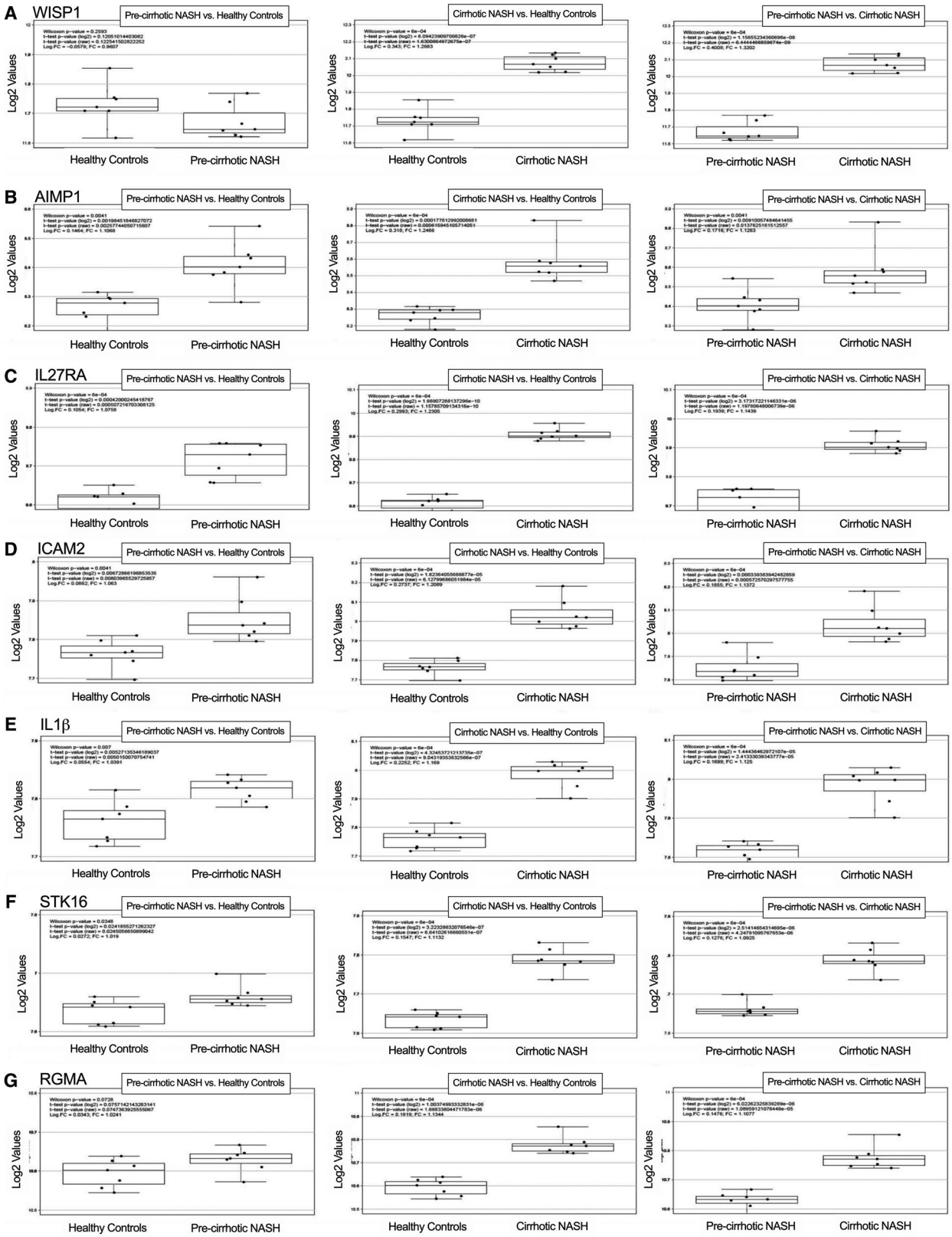
A
WISP1
Pre-cirrhotic NASH vs. Healthy Controls
Cirrhotic NASH vs. Healthy Controls
Pre-cirrhotic NASH vs. Cirrhotic NASH
B
AIMP1
C
IL27RA
D
ICAM2
E
IL1β
F
STK16
G
RGMA
Log2 Values
Healthy Controls
Pre-cirrhotic NASH
Cirrhotic NASH

FIG. 6. Pairwise comparisons of different levels of circulating EV proteins in a validation cohort of patients with cirrhotic NASH, patients with precirrhotic NASH, and healthy controls. Boxplots of pairwise comparisons of the top seven highest expressed circulating EV proteins isolated from patients with cirrhotic NASH, patients with precirrhotic NASH, and healthy controls. Data are reported as log2FC for WISP1 (A), AIMP1 (B), IL27RA (C), ICAM2 (D), IL1β (E), STK16 (F), and RGMA (G) for the three comparisons: patients with precirrhotic NASH versus healthy controls (left), patients with cirrhotic NASH versus healthy controls (center), and patients with precirrhotic NASH versus patients with cirrhotic NASH (right). Wilcoxon test (nonparametric, comparing the distributions of pairwise cohorts) and a regular Student *t* test (comparing means of raw and log2 values) were used to generate the *P* values reported in the boxplots.

the levels of immune cell-derived EVs in patients with NASH,[30] we used an unbiased approach and characterized total circulating EVs as well as EVs derived from hepatocytes, as they represent the most abundant cell in the liver and are particularly affected by lipid-induced toxicity.[30] More recent studies on patient cohorts provided insights on the bioavailability of circulating EVs in various biofluids and, as a consequence, on their potential use as biomarkers for various diseases such as cancer,[10,21] cardiovascular diseases,[31] renal disease[20] and liver disease.[30,32] However, studies that investigate the EV dynamics, protein cargo, and performance as potential biomarkers in well-characterized and liver biopsy-proven cohorts of patients with NASH are currently not available.[13,16] For this reason, we isolated circulating EVs from a well-characterized cohort of patients with histologically confirmed advanced NASH-associated fibrosis. Considering the heterogeneity of circulating EVs and challenges of EV isolation from biofluids, we performed a full characterization of our EV samples, including physical and molecular assessments, to provide evidence on the properties of our EV population and confirm the presence of EVs in our samples before any further analysis of EV quantity and cargo. Physical and molecular characterization of EVs identified elevated levels of circulating EVs in advanced NASH samples compared with healthy controls. Isolated circulating EVs expressed common EV markers, such as Alix, TSG101 and CD63, and elicit similar size. Several studies have shown that circulating EVs shuttle bioactive molecules from the parental cell or tissue of origin, and liver cells are not an exception. Hepatocytes, like all other liver cells, produce and release EVs,[33-35] which contain hepatocyte markers ASGPR1 and SLC27A5.[13,36] Based on these results, measurement of hepatocyte-derived circulating EVs may be a more sensitive, robust, and disease-specific approach than measuring total EVs. We indeed confirmed that approximately 20% of total circulating EVs derive from hepatocytes and that ASGPR1-positive, but not SLC27A5-positive, hepatocyte-specific EV amount progressively increases with disease severity and significantly correlates with clinical characteristics of NASH, including fibrosis stage, noninvasive markers of fibrosis (e.g., ELF test, FibroTest, NAFLD Fibrosis Score), bilirubin, platelet count, and HVPG. The worse correlation of SLC27A5-positive EVs and NASH/cirrhosis may be associated with fat loss during transition to cirrhosis and lower hepatocyte specificity of this enzyme, which is expressed in other extrahepatic tissues, such as lungs and gallbladder. Notably, ASGPR1+ hepatocyte EVs significantly correlated with HVPG, a variable of established assessment of portal hypertension, and were able to reliably identify patients with HVPG of 10 mmHg or higher, which has been identified has the clinically significant threshold for the diagnosis of portal hypertension. An elegant study by Payancé et al.[37] also reported a correlation between hepatocyte-derived EV (defined based on the presence of cytokeratin-18 within EVs) levels with HVPG. Our results provide further evidence that ASGPR1+ hepatocyte-specific EVs may represent a surrogate noninvasive biomarker of portal hypertension in patients with cirrhotic NASH. If confirmed, these findings may support clinical utility of ASGPR1-positive EVs as potential alternative to invasive HVPG. A major hurdle in translating biomarker research studies into clinically useful assays is a lack of reproducibility and rigorous criteria for reporting of potential NASH biomarkers. For this study, we adopted a multimarker approach by identifying and validating statistically a manageable number of EV proteins that can provide higher sensitivity and specificity than individual markers. Analysis of the circulating EV protein cargo in each study group identified unique protein signatures that were validated and that carry strong prognostic power, particularly to separate healthy controls and patients with precirrhotic NASH from patients with cirrhotic NASH. Unfortunately, independent proteomics analysis of EVs isolated from patients with advanced NASH are currently limited

or not available. However, proteomics analysis of EVs isolated from experimental murine models of NASH reported similar signatures or single analytes that were also found in our report. Larger and additional studies will be required to confirm our findings. An important element for our study was to avoid any potential contamination of plasma proteins or lipoproteins in our EV samples. Therefore, for EV isolation, we combined differential centrifugation with size-exclusion chromatography, which has been shown to provide purer EV samples.[22] Interestingly, our proteomics array, which included over 1,300 unique analytes, identified a large number of proteins differentially expressed in EVs from healthy individuals, patients with precirrhotic NASH, and patients with cirrhotic NASH, suggesting that protein cargo of circulating EVs is unique for each NASH stage and that these stage-specific protein signatures may have utility as liquid biopsies for diagnosis of patients with NASH. To further improve the robustness of our findings, we conducted extensive validation analyses using an extension of the kTSP to develop understandable and powerful EV-based proteomics signatures. Our analysis showed that selected protein pairs warrant strong predictive power not only for advanced NASH but also for differentiating precirrhotic and cirrhotic NASH. Additional statistical authentication of our data confirmed associations between identified circulating EV protein signatures with precirrhotic and cirrhotic NASH samples. Specifically, pair-wise comparisons showed that EV proteins such as WISP1, AIMP1, IL27RA, ICAM2, IL1β, STK16, and RGMA can reliably differentiate healthy controls from patients with precirrhotic and cirrhotic NASH. Although the specific roles of these proteins in the progression of NASH are not fully understood, it is known that they are involved in processes relevant to NASH progression, such as inflammation (IL1β, AIMP1, IL27RA, ICAM2), cell death (WISP1), wound healing (AIMP1), vesicle trafficking, and the transforming growth factor β/SMAD signaling pathway (STK16, RGMA). Despite the statistically powerful performance of the identified EV-protein signatures in discriminating healthy individuals from individuals with advanced NASH or patients with precirrhotic NASH from cirrhotic NASH, these results will require validation by independent groups. In addition, further studies in cohorts including patients with early NASH and isolated fatty liver, as well as non-NASH liver disease controls, will provide important information regarding the utility of EV assessment for distinguishing the full spectrum of patients with NAFLD.

Study Limitations

The limitations of this study include the relatively low number of samples analyzed and the lack of samples from patients with early NASH. This is also reflected in the relatively large confidence intervals of the AUROC analyses found in the proteomic-based studies. Future validation using larger number of patient samples are therefore needed to confirm the EV-protein signatures identified in our study utility as a NASH liquid biopsy.

Acknowledgment: The authors thank Vanessa Taupin of the UCSD Electron Microscopy Facility for the technical expertise and help with electron microscopy imaging of EVs.

REFERENCES

1) Younossi ZM, Koenig AB, Abdelatif D, Fazel Y, Henry L, Wymer M. Global epidemiology of nonalcoholic fatty liver disease—meta-analytic assessment of prevalence, incidence, and outcomes. Hepatology 2016;64:73-84.
2) Charlton MR, Burns JM, Pedersen RA, Watt KD, Heimbach JK, Dierkhising RA. Frequency and outcomes of liver transplantation for nonalcoholic steatohepatitis in the United States. Gastroenterology 2011;141:1249-1253.
3) Wong RJ, Aguilar M, Cheung R, Perumpail RB, Harrison SA, Younossi ZM, et al. Nonalcoholic steatohepatitis is the second leading etiology of liver disease among adults awaiting liver transplantation in the United States. Gastroenterology 2015;148:547-555.
4) Doycheva I, Watt KD, Rifai G, Abou Mrad R, Lopez R, Zein NN, et al. Increasing burden of chronic liver disease among adolescents and young adults in the USA: a silent epidemic. Dig Dis Sci 2017;62:1373-1380.
5) Younossi Z, Anstee QM, Marietti M, Hardy T, Henry L, Eslam M, et al. Global burden of NAFLD and NASH: trends, predictions, risk factors and prevention. Nat Rev Gastroenterol Hepatol 2018;15:11-20.
6) Singh S, Allen AM, Wang Z, Prokop LJ, Murad MH, Loomba R. Fibrosis progression in nonalcoholic fatty liver vs nonalcoholic steatohepatitis: a systematic review and meta-analysis of paired-biopsy studies. Clin Gastroenterol Hepatol 2015;13:643-654: e641-649; quiz e639-640.
7) Goldberg D, Ditah IC, Saeian K, Lalehzari M, Aronsohn A, Gorospe EC, et al. Changes in the prevalence of hepatitis C virus infection, nonalcoholic steatohepatitis, and alcoholic liver disease among patients with cirrhosis or liver failure on the waitlist for liver transplantation. Gastroenterology 2017;152:1090-1099.e1091.
8) McGill DB, Rakela J, Zinsmeister AR, Ott BJ. A 21-year experience with major hemorrhage after percutaneous liver biopsy. Gastroenterology 1990;99:1396-1400.

9) Wong VW, Adams LA, de Ledinghen V, Wong GL, Sookoian S. Noninvasive biomarkers in NAFLD and NASH—current progress and future promise. Nat Rev Gastroenterol Hepatol 2018;15:461-478.
10) Skog J, Wurdinger T, van Rijn S, Meijer DH, Gainche L, Sena-Esteves M, et al. Glioblastoma microvesicles transport RNA and proteins that promote tumour growth and provide diagnostic biomarkers. Nat Cell Biol 2008;10:1470-1476.
11) van Niel G, D'Angelo G, Raposo G. Shedding light on the cell biology of extracellular vesicles. Nat Rev Mol Cell Biol 2018;19:213-228.
12) Eguchi A, Kostallari E, Feldstein AE, Shah VH. Extracellular vesicles, the liquid biopsy of the future. J Hepatol 2019;70:1292-1294.
13) Povero D, Eguchi A, Li H, Johnson CD, Papouchado BG, Wree A, et al. Circulating extracellular vesicles with specific proteome and liver microRNAs are potential biomarkers for liver injury in experimental fatty liver disease. PLoS One 2014;9:e113651.
14) Harrison SA, Abdelmalek MF, Caldwell S, Shiffman ML, Diehl AM, Ghalib R, et al. Simtuzumab is ineffective for patients with bridging fibrosis or compensated cirrhosis caused by nonalcoholic steatohepatitis. Gastroenterology 2018;155:1140-1153.
15) Lane RE, Korbie D, Trau M, Hill MM. Purification protocols for extracellular vesicles. Methods Mol Biol 2017;1660:111-130.
16) Saha B, Momen-Heravi F, Furi I, Kodys K, Catalano D, Gangopadhyay A, et al. Extracellular vesicles from mice with alcoholic liver disease carry a distinct protein cargo and induce macrophage activation through heat shock protein 90. Hepatology 2018;67:1986-2000.
17) Marchionni L, Afsari B, Geman D, Leek JT. A simple and reproducible breast cancer prognostic test. BMC Genom 2013;14:336.
18) Tan AC, Naiman DQ, Xu L, Winslow RL, Geman D. Simple decision rules for classifying human cancers from gene expression profiles. Bioinformatics 2005;21:3896-3904.
19) Chen J, Hu C, Pan P. Extracellular vesicle microRNA transfer in lung diseases. Front Physiol 2017;8:1028.
20) Erdbrugger U, Le TH. Extracellular vesicles in renal diseases: more than novel biomarkers? J Am Soc Nephrol 2016;27:12-26.
21) Hornick NI, Huan J, Doron B, Goloviznina NA, Lapidus J, Chang BH, et al. Serum exosome microRNA as a minimally-invasive early biomarker of AML. Sci Rep 2015;5:11295.
22) Lozano-Ramos I, Bancu I, Oliveira-Tercero A, Armengol MP, Menezes-Neto A, Del Portillo HA, et al. Size-exclusion chromatography-based enrichment of extracellular vesicles from urine samples. J Extracell Vesicles 2015;4:27369.
23) Noerholm M, Balaj L, Limperg T, Salehi A, Zhu LD, Hochberg FH, et al. RNA expression patterns in serum microvesicles from patients with glioblastoma multiforme and controls. BMC Cancer 2012;12:22.
24) Lozano-Andres E, Libregts SF, Toribio V, Royo F, Morales S, Lopez-Martin S, et al. Tetraspanin-decorated extracellular vesicle-mimetics as a novel adaptable reference material. J Extracell Vesicles 2019;8:1573052.
25) Colombo M, Moita C, van Niel G, Kowal J, Vigneron J, Benaroch P, et al. Analysis of ESCRT functions in exosome biogenesis, composition and secretion highlights the heterogeneity of extracellular vesicles. J Cell Sci 2013;126:5553-5565.
26) Enooku K, Tsutsumi T, Kondo M, Fujiwara N, Sasako T, Shibahara J, et al. Hepatic FATP5 expression is associated with histological progression and loss of hepatic fat in NAFLD patients. J Gastroenterol 2020;55:227-243.
27) Yanez-Mo M, Siljander PR, Andreu Z, Zavec AB, Borras FE, Buzas EI, et al. Biological properties of extracellular vesicles and their physiological functions. J Extracell Vesicles 2015;4:27066.
28) Tkach M, Thery C. Communication by extracellular vesicles: where we are and where we need to go. Cell 2016;164:1226-1232.
29) Maas SLN, Breakefield XO, Weaver AM. Extracellular vesicles: unique intercellular delivery vehicles. Trends Cell Biol 2017;27:172-188.
30) Kornek M, Lynch M, Mehta SH, Lai M, Exley M, Afdhal NH, et al. Circulating microparticles as disease-specific biomarkers of severity of inflammation in patients with hepatitis C or nonalcoholic steatohepatitis. Gastroenterology 2012;143:448-458.
31) Dickhout A, Koenen RR. Extracellular vesicles as biomarkers in cardiovascular disease; chances and risks. Front Cardiovasc Med 2018;5:113.
32) Bala S, Petrasek J, Mundkur S, Catalano D, Levin I, Ward J, et al. Circulating microRNAs in exosomes indicate hepatocyte injury and inflammation in alcoholic, drug-induced, and inflammatory liver diseases. Hepatology 2012;56:1946-1957.
33) Royo F, Schlangen K, Palomo L, Gonzalez E, Conde-Vancells J, Berisa A, et al. Transcriptome of extracellular vesicles released by hepatocytes. PLoS One 2013;8:e68693.
34) Rodriguez-Suarez E, Gonzalez E, Hughes C, Conde-Vancells J, Rudella A, Royo F, et al. Quantitative proteomic analysis of hepatocyte-secreted extracellular vesicles reveals candidate markers for liver toxicity. J Proteomics 2014;103:227-240.
35) Masyuk AI, Masyuk TV, Larusso NF. Exosomes in the pathogenesis, diagnostics and therapeutics of liver diseases. J Hepatol 2013;59:621-625.
36) Conde-Vancells J, Rodriguez-Suarez E, Embade N, Gil D, Matthiesen R, Valle M, et al. Characterization and comprehensive proteome profiling of exosomes secreted by hepatocytes. J Proteome Res 2008;7:5157-5166.
37) Payance A, Silva-Junior G, Bissonnette J, Tanguy M, Pasquet B, Levi C, et al. Hepatocyte microvesicle levels improve prediction of mortality in patients with cirrhosis. Hepatology 2018;68:1508-1518.
38) Daskalow K, Rohwer N, Raskopf E, Dupuy E, Kuhl A, Loddenkemper C, et al. Role of hypoxia-inducible transcription factor 1alpha for progression and chemosensitivity of murine hepatocellular carcinoma. J Mol Med (Berl) 2010;88:817-827.
39) Cotton RJ, Graumann J. readat: an R package for reading and working with SomaLogic ADAT files. BMC Bioinformatics 2016;17:201.
40) Wang X, Chen Z, Mishra AK, Silva A, Ren W, Pan Z, et al. Chemotherapy-induced differential cell cycle arrest in B-cell lymphomas affects their sensitivity to Wee1 inhibition. Haematologica 2018;103:466-476.
41) Ritchie ME, Phipson B, Wu D, Hu Y, Law CW, Shi W, et al. Limma powers differential expression analyses for RNA-sequencing and microarray studies. Nucleic Acids Res 2015;43:e47.
42) Afsari B, Fertig EJ, Geman D, Marchionni L. SwitchBox: an R package for k-Top Scoring Pairs classifier development. Bioinformatics 2015;31:273-274.

Supporting Information

Additional Supporting Information may be found at onlinelibrary.wiley.com/doi/10.1002/hep4.1556/suppinfo.